

High-frequency microwave cavity design for high-mass dark matter axion searches

Chi Zhang, Jia Wang, Chunguang Li, Shiguang Chen, Hang Cheng, Liang Sun, and Yun Wu

Citation: Chin. Phys. B, 2024, 33 (**5**): 054211. DOI: 10.1088/1674-1056/ad34ca
Journal homepage: http://cpb.iphy.ac.cn; http://iopscience.iop.org/cpb

What follows is a list of articles you may be interested in

Broadband bidirectional Brillouin-Raman random fiber laser with ultra-narrow linewidth

Qian Yang(杨茜), Yang Li(李阳), Hui Zou(邹辉), Jie Mei(梅杰), En-Ming Xu(徐恩明), and Zu-Xing Zhang(张祖兴)
Chin. Phys. B, 2024, 33 (**2**): 024206. DOI: 10.1088/1674-1056/ad09cb

Tunable magnomechanically induced transparency and fast-slow light in a hybrid cavity magnomechanical system

Qinghong Liao(廖庆洪), Kun Peng(彭坤), and Haiyan Qiu(邱海燕)
Chin. Phys. B, 2023, 32 (**5**): 054205. DOI: 10.1088/1674-1056/acaf2b

Degenerate cascade fluorescence: Optical spectral-line narrowing via a single microwave cavity

Liang Hu(胡亮), Xiang-Ming Hu(胡响明), and Qing-Ping Hu(胡庆平)
Chin. Phys. B, 2021, 30 (**6**): 064211. DOI: 10.1088/1674-1056/abd76b

ontrol of microwave signals using bichromatic electromechanically induced transparency in multimode circuit electromechanical systems

Cheng Jiang(江成), Yuanshun Cui(崔元顺), Xintian Bian(边心田), Xiaowei Li(李晓薇), Guibin Chen(陈贵宾)
Chin. Phys. B, 2016, 25 (**5**): 054204. DOI: 10.1088/1674-1056/25/5/054204

Controllable optical response in hybrid opto-electromechanical systems

Jiang Cheng (江成), Cui Yuan-Shun (崔元顺), Liu Hong-Xiang (刘洪香), Li Xiao-Wei (李晓薇), Chen Gui-Bin (陈贵宾)
Chin. Phys. B, 2015, 24 (**5**): 054206. DOI: 10.1088/1674-1056/24/5/054206

INSTRUMENTATION AND MEASUREMENT

High-frequency microwave cavity design for high-mass dark matter axion searches

Chi Zhang(张驰)[1,2], Jia Wang(王佳)[1], Chunguang Li(李春光)[1], Shiguang Chen(陈石广)[1,2], Hang Cheng(程航)[1,2], Liang Sun(孙亮)[1,3], and Yun Wu(吴云)[1,2,4,†]

[1] *Beijing National Laboratory for Condensed Matter Physics, Institute of Physics, Chinese Academy of Sciences, Beijing* 100190, *China*
[2] *University of Chinese Academy of Sciences, Beijing* 100049, *China*
[3] *Songshan Lake Materials Laboratory, Dongguan* 523808, *China*
[4] *Hefei National Laboratory, Hefei* 230088, *China*

(Received 1 February 2024; revised manuscript received 14 March 2024; accepted manuscript online 18 March 2024)

The haloscope based on the TM_{010} mode cavity is a well-established technique for detecting QCD axions. However, the method has limitations in detecting high-mass axion due to significant volume loss in the high-frequency cavity. Utilizing a higher-order mode cavity can effectively reduce the volume loss of the high-frequency cavity. The rotatable dielectric pieces as a tuning mechanism can compensate for the degradation of the form factor of the higher-order mode. Nevertheless, the introduction of dielectric causes additional volume loss. To address these issues, this paper proposes a novel design scheme by adding a central metal rod to the higher-order mode cavity tuned by dielectrics, which improves the performance of the haloscope due to the increased effective volume of the cavity detector. The superiority of the novel design is demonstrated by comparing its simulated performance with previous designs. Moreover, the feasibility of the scheme is verified by the full-wave simulation results of the mechanical design model.

Keywords: axion, haloscope, microwave cavity

PACS: 42.60.Da, 95.35.+d

DOI: 10.1088/1674-1056/ad34ca

1. Introduction

The axion has emerged as the most promising candidate for the major component of cold dark matter in recent years.[1] Hence, the detection of axions is significant in cosmology and particle physics.

Several detectors for searching axions have been constructed based on the haloscope proposed by Sikivie in 1983.[2] The scheme involves a resonant cavity penetrated by a strong magnetic field that enables the conversion of axions into photons. The conversion signal is significantly enhanced when the resonant frequency f_c matches the axion frequency $f_a \approx m_a c^2/h$, where m_a is the axion mass, c is the velocity of the light in the vacuum, and h is the Plank's constant. As the axion mass remains unknown, the microwave cavity with a continuously tunable frequency range is in urgent need for detecting prospective axion signals covering a wide range of mass. The axion-to-photon conversion power produced in the cavity operating in the specific mode TM_{mnp} or TE_{mnp} is defined as[3]

$$P_{mnp} = g_{a\gamma\gamma}^2 \frac{\rho_a}{m_a} B_0^2 V C_{mnp} \frac{Q_L Q_a}{Q_L + Q_a}, \tag{1}$$

where $g_{a\gamma\gamma}$ is the axion-to-photon coupling, ρ_a is the local mass density of the axion field, B_0 is the magnetic induction intensity of the external static field, V is the volume of the cavity, Q_L is the loaded quality factor of the cavity, Q_a is the axion quality factor ($\sim 10^6$)[4], and C_{mnp} is the mode-dependent form factor of the cavity where subscripts m, n, and p are the azimuthal, radial, and longitudinal mode numbers of TE_{mnp} or TM_{mnp} mode cavity, respectively.

The most mature and sensitive axion haloscope experiment is the Axion Dark Matter eXperiment (ADMX).[5] The original scanning range of axion mass in ADMX covered 1.9–3.69 μeV (corresponding to 0.46–0.89 GHz of cavity resonant frequency)[5–7] and has been currently extended to 6.2 μeV (1.5 GHz).[8] Based on the analysis of the experimental results, the low-mass parameter space mentioned above has been excluded with a high confidence level. In addition, recent theoretical predictions[9,10] regarding the axion mass have motivated the search for high-mass axions, leading to high-frequency cavity experiments such as the high-masse At Yale Sensitive to Axion Cold dark matter (HAYSTAC) experiment.[11] Therefore, our study focuses on the scanning frequency range of 8–10 GHz to search for higher mass axions.

Detecting high-mass axions necessitates designing high-frequency cavity resonators, which pose challenges. The most prominent issue is the significant volume loss for high-frequency cavities, which decreases the axion-to-photon conversion power and scan rate. Various methods have been proposed to address it.[11–14] For example, HAYSTAC em-

†Corresponding author. E-mail: wuyun@iphy.ac.cn

© 2024 Chinese Physical Society and IOP Publishing Ltd

ployed a thick metal rod to reduce volume loss and enable wide-range frequency tuning.[11] Due to limitations imposed by cavity dimensions and degradation of quality factor, this method is restricted in compensating for the volume loss of high-frequency microwave cavities. Moreover, the displacement of the thick rod along the radius breaks the azimuthal symmetry of the electromagnetic field distribution, which results in a pronounced reduction of the form factor. Another approach involves the cavity operating in high-order resonant modes, such as TM_{020} and TM_{030} modes. Despite the high quality factor (Q-factor) of these modes, the presence of out-of-phase components of the electric field decreases the form factor. Kim *et al*. utilized rotatable dielectric pieces inserted in the proper position to enhance the form factor by suppressing the out-of-phase component.[15] Nevertheless, the insertion of dielectrics reduces the resonant frequency of the microwave cavity, thereby introducing additional volume loss. Additionally, the rotation angle is limited, which restricts the accessible tuning range.

This paper presents a comprehensive solution inspired by the schemes proposed in Refs. [11,15] to achieve improved performance. The rotatable dielectric pieces enable flexibility and ease of tuning and the metal rod inserted at the center of the cavity compensates for the resulting volume loss. The optimization of the structure of dielectrics as the tuning mechanism was performed using electromagnetic (EM) simulation software. Moreover, a comparative analysis was conducted to demonstrate the superiority of the proposed method over the two previous designs. Finally, the feasibility of the proposed scheme was verified through the mechanical design and full-wave simulation of the novel microwave cavity.

2. Cavity performance evaluation

As mentioned above, the axion mass is presently unknown, necessitating the tunability of the search mode frequency in the haloscope. To detect axions, the search mode frequency of the microwave cavity in a haloscope is first tuned to an initial value. The signal produced in the cavity is measured within a specified scan integration time. Subsequently, the search mode frequency is tuned in small increments, and the measurement process is repeated. The signal-to-noise ratio of experimental observations is crucial for identifying axion signals from noise fluctuations, which can be determined as[16]

$$\mathrm{SNR} = \frac{P_{mnp}}{k_\mathrm{B} T_\mathrm{n}} \sqrt{t/b}, \tag{2}$$

where t is the scan integration time, b is the bandwidth of signal, k_B is the Boltzmann's constant, and T_n is the system noise temperature. According to Eq. (2), the signal-to-noise ratio can be improved by enhancing the produced signal power, increasing the scan integration time, and decreasing the noise temperature of the system. However, the scanning integration time for a single frequency point is limited, originating from the fact that the axion detectors should be tuned over a sufficiently wide frequency range within a reasonable operating period (approximately a few months to several years). To cover a wide range of axion masses within the operating period of the detector, the scan rate of the haloscope should be significantly elevated. Therefore, under a given sensitivity, the scan rate factor is regarded as the underlying figure of merit of the haloscope. If Q_a is larger than Q_L, the scan rate factor of the haloscope is given by[3]

$$\frac{\mathrm{d}f}{\mathrm{d}t} \approx \left(\frac{1}{\mathrm{SNR}}\right)^2 \left(\frac{1}{k_\mathrm{B} T_\mathrm{n}}\right)^2 \frac{g_{a\gamma\gamma}^4 \rho_\mathrm{a}^2}{m_\mathrm{a}^2} B_0^4 V^2 C_{mnp}^2 Q_\mathrm{L} Q_\mathrm{a}. \tag{3}$$

The loaded quality factor can be further expressed as

$$Q_\mathrm{L} = \frac{Q}{1+\beta}, \tag{4}$$

where Q is the unloaded quality factor, and β is the coupling coefficient whose typical value is 1.

According to Eq. (3), assuming that all other parameters remain constant, enhancing the scan rate factor necessitates a significant decrease in signal-to-noise ratio, which is not conducive to detecting axion signal. Therefore, the axion search utilizing the haloscope requires a trade-off between noise-to-signal ratio and scan rate. This contradiction can be mitigated by increasing the scan rate factor through optimization of other parameters. For example, optimizing the design of the microwave cavity in a haloscope is an effective method. By extracting the physical quantities related to the microwave cavity specified in Eq. (3), the figure of merit quantitatively evaluating the performance of the microwave cavity for axion search can be determined as

$$\mathrm{FOM} = {C_{mnp}}^2 V^2 Q. \tag{5}$$

The scan rate factor can be improved by enhancing the FOM of the microwave cavity. Therefore, optimizing the design of the microwave cavity is accessible to enhance the detection efficiency of the haloscope, leading to a wider scan rate within a limited operation period. The corresponding criteria for the performance evaluation of microwave cavities are discussed below in detail.

2.1. Form factor

The form factor C_{mnp} can be calculated as

$$C_{mnp} = \frac{\left| \int \mathrm{d}^3 x \boldsymbol{B}_0 \cdot \boldsymbol{E}_{mnp}(\boldsymbol{x}) \right|^2}{{B_0}^2 V \int \mathrm{d}^3 x \varepsilon_\mathrm{r}(\boldsymbol{x}) \left| \boldsymbol{E}_{mnp}(\boldsymbol{x}) \right|^2}, \tag{6}$$

where $\boldsymbol{E}_{mnp}(\boldsymbol{x})$ is the electric field strength of the resonant mode TM_{mnp} or TE_{mnp}, $\varepsilon_\mathrm{r}(\boldsymbol{x})$ is the relative permittivity of

the dielectrics filled in the cavity, and V is the volume as referred to Eq. (1). The axion signal exhibits significant overlaps with the TM_{0n0}-like mode where the dominant electric field component aligns with the length direction of the cylinder. Therefore, the microwave cavity usually operates in TM_{0n0}-like modes. The form factor is inaccessible for measurement. Thus, electromagnetic (EM) simulation is the only method for determining the form factor.

2.2. Cavity volume

The volume of the microwave cavity V is defined as

$$V = \pi R^2 L, \tag{7}$$

where R and L are the radius and length of the cylindrical cavity, respectively. The radius R of an air-filled cylindrical cavity can be calculated by

$$R = \frac{c\chi_{0n}}{2\pi f_{0n0}}, \tag{8}$$

where c is the speed of light, χ_{0n} is the n-th root of the zeroth order Bessel function (J_0), and f_{0n0} is the resonate frequency of the TM_{0n0} mode. The length is independent of the frequency but constrained by the aspect ratio L/R which should be no more than 5 to reduce the intruding modes density. Thus, the volume of an empty cavity with a fixed aspect ratio is inversely proportional to the third power of the resonant frequency. To search for high-mass axions, the resonant cavity must operate at a high frequency, which limits its volume according to Eq. (8). Therefore, optimizing the design of high-frequency cavities to compensate for volume loss is desirable.

Based on the form factor and cavity volume, the effective volume $V_{\rm eff}$ is further proposed to evaluate the cavity performance more comprehensively, which is defined as the product of form factor and cavity[17]

$$V_{\rm eff} = C_{mnp} V. \tag{9}$$

2.3. Quality factor

The unloaded quality factor Q is related to the ratio of energy storage to power loss, which is given by

$$Q = \frac{G}{R_{\rm s}} = \frac{\omega}{R_{\rm s}} \frac{\int_V \varepsilon(\boldsymbol{x}) \left|\boldsymbol{E}_{mnp}(\boldsymbol{x})\right|^2 {\rm d}V}{\int_S |\boldsymbol{H}_{\rm t}|^2 {\rm d}S}, \tag{10}$$

where $\boldsymbol{H}_{\rm t}$ is the tangential component of magnetic strength in the metallic surface, $R_{\rm s}$ is the surface resistance of the metal enclosure, $\varepsilon(\boldsymbol{x})$ is the permittivity of the dielectric filled in the cavity, and ω is the resonant angular frequency.

2.4. Tunability

The microwave cavity detectors are expected to have a wide frequency-tuning range to scan across a broad range of axion mass. Tunability also serves as a vital criterion for cavity performance. Therefore, a more comprehensive evaluation indicator can be defined as FOMF, which is expressed as[15]

$$\text{FOMF} = \int_{\Delta f} \text{FOM}\, {\rm d}f. \tag{11}$$

3. Design and simulation

The proposed cavity detector comprises a cylindrical cavity operating in the TM_{030} mode, a metal rod, and rotatable dielectric pieces. The dielectric pieces consist of two layers: an inner layer with inner radius $r_{\rm i}$ and outer radius $r_{\rm c}$, and an outer layer with inner radius $r_{\rm c}$ and outer radius $r_{\rm o}$. The optimal segment of dielectric pieces is suggested to be six to achieve the excellent performance of the cavity detector.[15] The synchronous rotation of the dielectric pieces in the inner layer implements frequency tuning by breaking the rotational symmetry (Fig. 1). The physical dimensions of the cylindrical cavity with a central metal rod inserted are chosen to meet the requirement of the operating frequency within the range of 8–10 GHz by theoretical calculations and simulations using CST Studio Suite (CST).[18] The general simulation procedure of a microwave cavity based on the CST software is shown in Fig. 2(a). To verify the reliability of the simulation presented in this paper, the microwave cavity described in Ref. [19] was simulated according to the process shown in Fig. 2(b). The simulated results of frequency, form factor and quality factor are consistent with those of Ref. [19] as shown in Figs. 2(c)–2(e), demonstrating the reliability of the simulation in this paper.

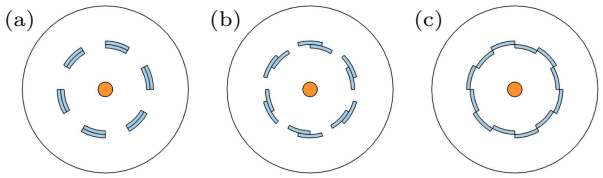


Fig. 1. Schematic structure of the proposed cavity detectors with different rotation angles of inner dielectric pieces: (a) 0°, (b) 15°, (c) 30°.

After demonstrating the reliability of simulation in this paper, the detailed process of the novel design is shown as follows. Firstly, the radius of the cylindrical cavity was determined as 45 mm, while the radius of the central metal rod was 4 mm. Then, considering the ease of fabrication in practice and the compromise between volume and intrude mode density, the aspect ratio L/R was selected as 4. Moreover, the rotatable dielectric pieces should be carefully designed. Due to several geometry parameters involved for dielectric pieces, the analysis for optimizing the dimensions of the rotatable dielectric pieces is complex. To simplify the analysis, a simulation was first conducted to determine the optimal size of a dielectric ring with only two size parameters, i.e., the inner radius $r_{\rm i}$ and the outer radius $r_{\rm o}$. The cylindrical cavity with a metal rod and a dielectric ring inserted was modeled as shown in Fig. 3.

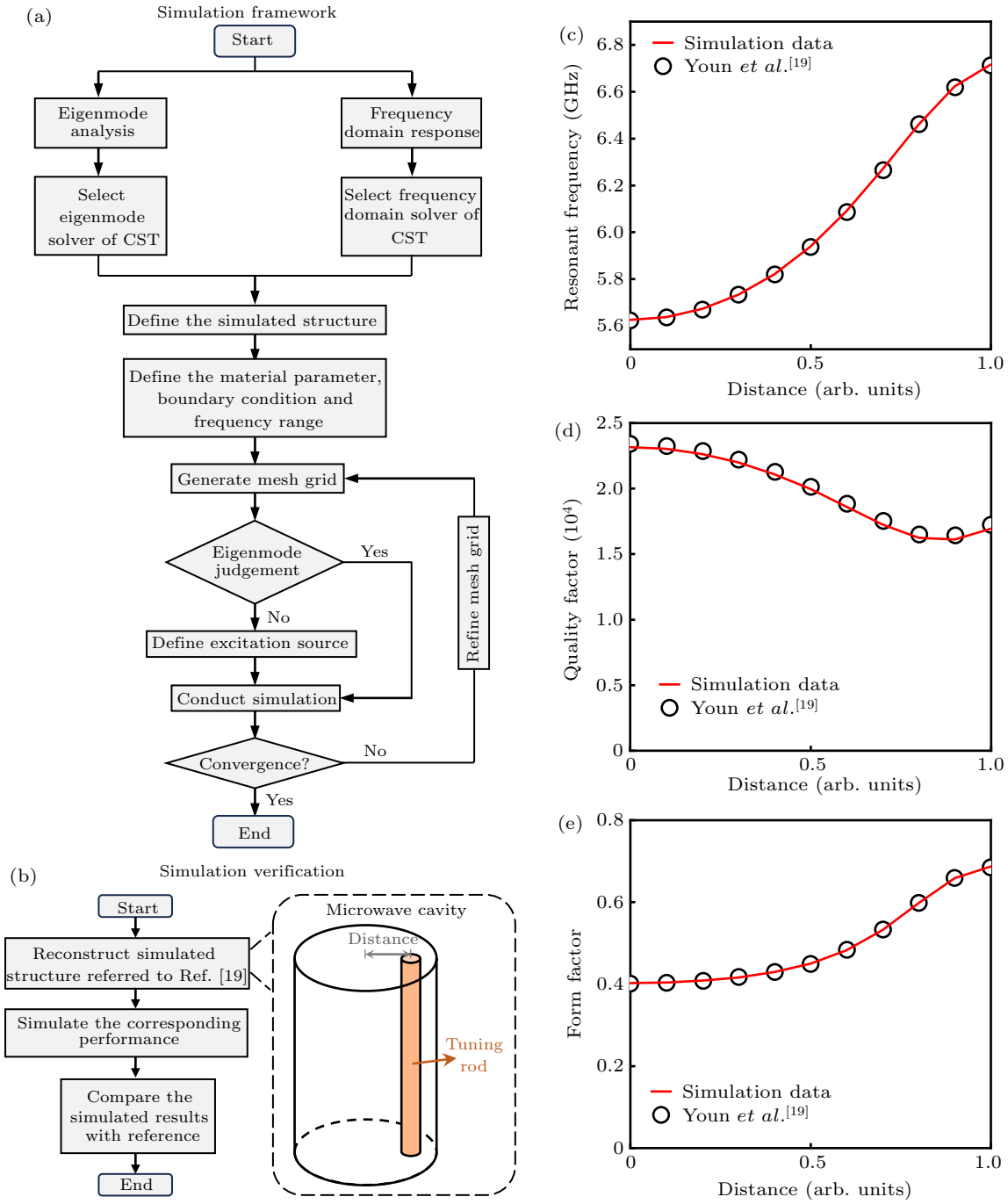


Fig. 2. (a) The general flow chart of simulation based on CST software. (b) The process of the verification of simulation reliability. The comparison of (c) frequency, (d) form factor, and (e) quality factor between simulated results in this work and reported in Ref. [19].

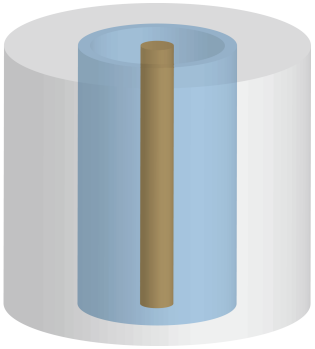


Fig. 3. The simplified model of the optimized design microwave cavity. A metal rod (in gold) and a dielectric ring (in cyan) are inserted into the cylindrical metallic enclosure (in gray).

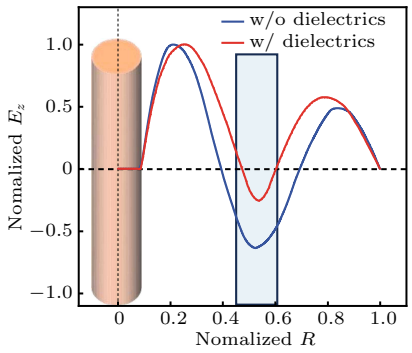


Fig. 4. The influence of the inserted dielectric ring (in cyan) on the radially distributed electric field of the microwave cavity operating in the TM_{030}-like mode with an inserted metal rod (in gold).

The dielectric ring was utilized to suppress the out-of-phase component of the electric field. Thus, the optimal central position of the dielectric ring ($r_c = (r_i + r_o)/2$) was selected as $r_c = 0.538R$, as illustrated in Fig. 4. The thickness of the dielectric ring ($d_t = r_o - r_i$) has been optimized to achieve the maximal value of FOM. The simulation results indicate that the optimal thickness is 4.6 mm, as depicted in Fig. 5.

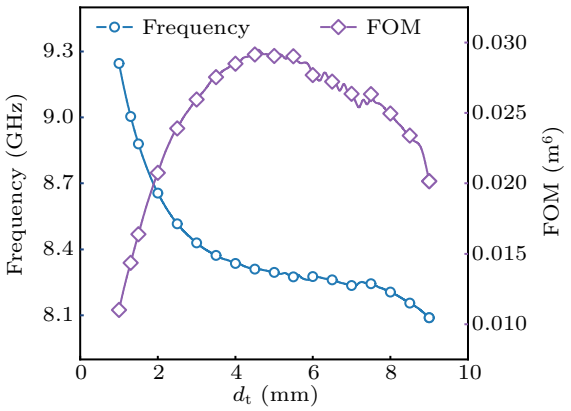


Fig. 5. Variation of FOM (purple square) and resonant frequency (blue circle) of the microwave cavity with the thickness of the dielectric ring inserted.

However, the analysis of the dielectric ring mentioned above is not sufficient to determine the optimal thickness of the rotatable dielectric pieces. The investigation of the tunability is also essential, as the thickness of the dielectric pieces also influences it. Further simulations were performed to compare the FOMF of the novel design cavity with different thicknesses of dielectric pieces. The estimated values of FOMF with different d_t of 3.8 mm, 4.6 mm, and 5.4 mm were 0.0093, 0.0101, and 0.0096, respectively (Fig. 6). Thus, the optimal thickness of the dielectric pieces was finally determined to be 4.6 mm. The electric field distribution of the microwave cavity operating in the TM_{030}-like mode was simulated while rotating the inner dielectric pieces (Fig. 7).

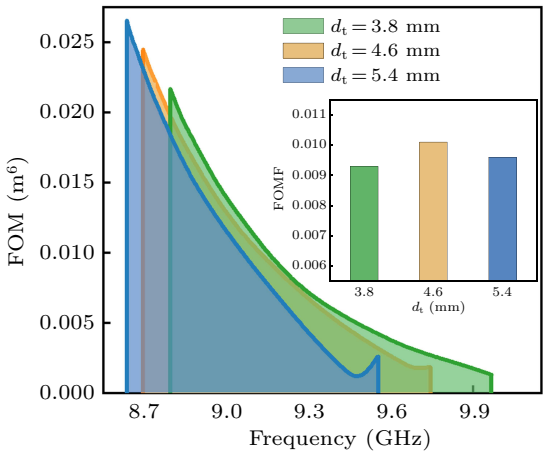


Fig. 6. Simulated variation of FOM versus frequency over the maximum tuning range for different thicknesses of inserted dielectric pieces.

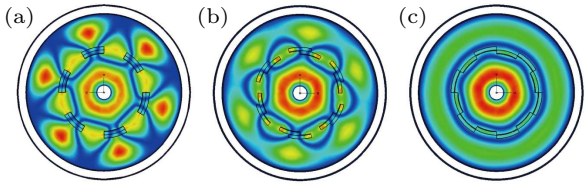


Fig. 7. The electric field distribution of the optimized design cavity corresponding to the different rotation angles of dielectrics as shown in Fig. 1.

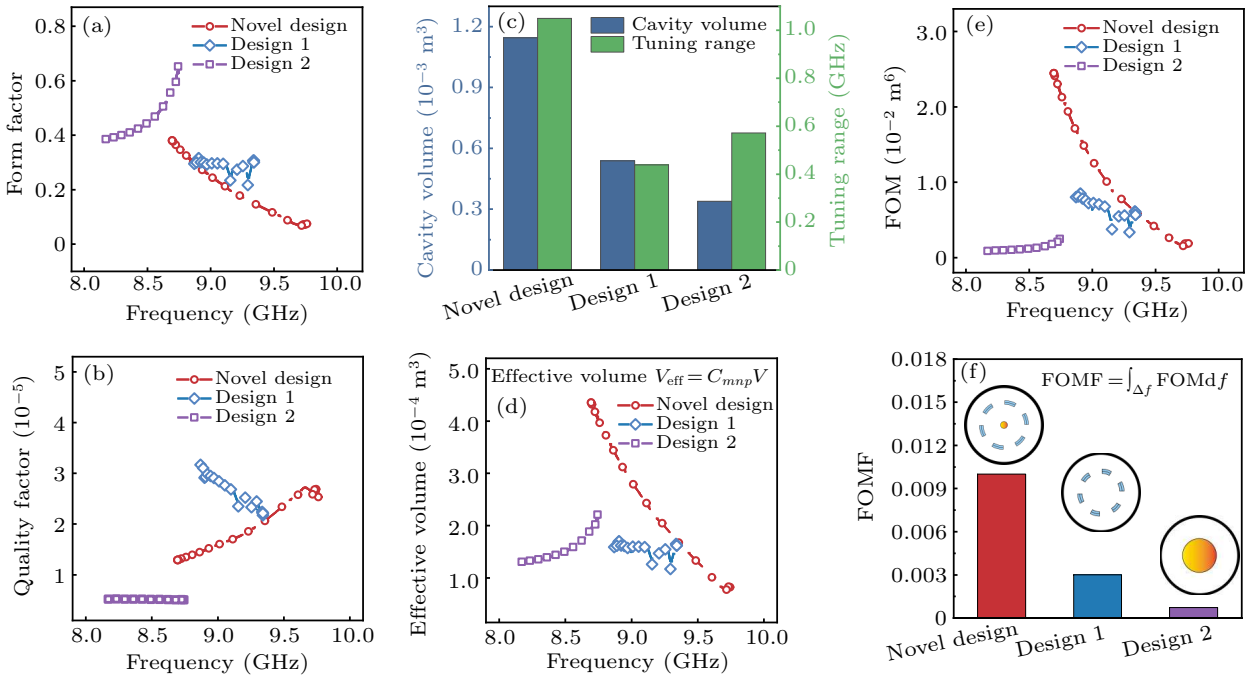


Fig. 8. Comparison of (a) form factor, (b) quality factor, (c) cavity volume, tuning range, (d) effective volume, (e) FOM, and (f) FOMF among three design schemes. Design 1 (blue rhombus) utilizes dielectric pieces as the tuning mechanism, design 2 (purple square) employs a thick metal rod as the tuning mechanism, while the novel design (red circle) presents a composite structure.

Inserting metals can increase the volume of the microwave cavity while maintaining the resonant frequency within the desired range. Therefore, it is expected that the novel design will enhance the volume of the microwave cavity for axion detection operating within a fixed frequency range. To further demonstrate the superiority of the novel design, two reference microwave cavities that also operate within 8–10 GHz were designed based on the methodology proposed in Refs. [11,15] and simulated for comparison. The radius of the one with a thick metal rod inserted was determined as 30 mm while the other with rotatable dielectric pieces inserted was determined as 35 mm. The aspect ratio of all microwave cavities was kept the same to maintain a comparable mode density. The eigenmode solver of CST[18] was used to simulate the performance of the microwave cavities in the three design schemes. The material of the cavity enclosure in the simulation model was set as copper with the anomalous skin effect to emulate a cryogenic environment for practical detector operation. Subsequently, a comprehensive comparison of the performance of the three design schemes was conducted, as depicted in Fig. 8. The cavity volume is significantly increased in the novel design compared with design 1 while maintaining comparable levels of form factor and quality factor (Figs. 8(a)–8(c)). Despite a slight degradation of form factor, the novel design improves both the cavity volume and quality factor of the cavity detector compared with design 2 (Figs. 8(a)–8(c)). The novel design significantly enhances the FOM of cavity detectors by increasing the effective volume, as illustrated in Figs. 8(d) and 8(e). Moreover, as shown in Fig. 8(f), the cavity detector in the novel design shows the highest FOMF, enabling detecting axions with higher detection efficiency and covering a wider mass range.

4. Mechanical design and full-wave simulation

The mechanical design model of the improved microwave cavity was constructed and simulated to exhibit the feasibility of the proposed design scheme. Copper was used for the metallic parts, while highly pure aluminum oxide ceramics (99.8% Al_2O_3, $\varepsilon_r = 9.85$) were chosen as the dielectric material. The cavity enclosure comprises three parts, each with a step edge to ensure good sealing (Fig. 9(a)). The inner radius and height of the cavity were set as 45 mm and 180 mm, respectively. The bottom endcap consisted of two parts. As illustrated in Fig. 9(b), a rotatable disk was embedded in the center of the base through a groove. The tuning mechanism consisted of an inner and an outer part. The outside dielectric cylinder was firmly attached to the base, while the inner one was securely attached to the rotatable disk, allowing it to rotate relative to the outer dielectric (Fig. 9(c)). A copper rod with a radius of 4 mm was mounted in the center of the cavity through the groove in the rotatable disk (Fig. 9(d)). The thin probe antennas were inserted into the cavity as excitation ports (Fig. 9(d)). To excite the TM_{030} mode, the axis of the probes must be parallel to the electric field of the TM_{030} mode cavity, and it was placed at the position with the maximum strength of the electric field.

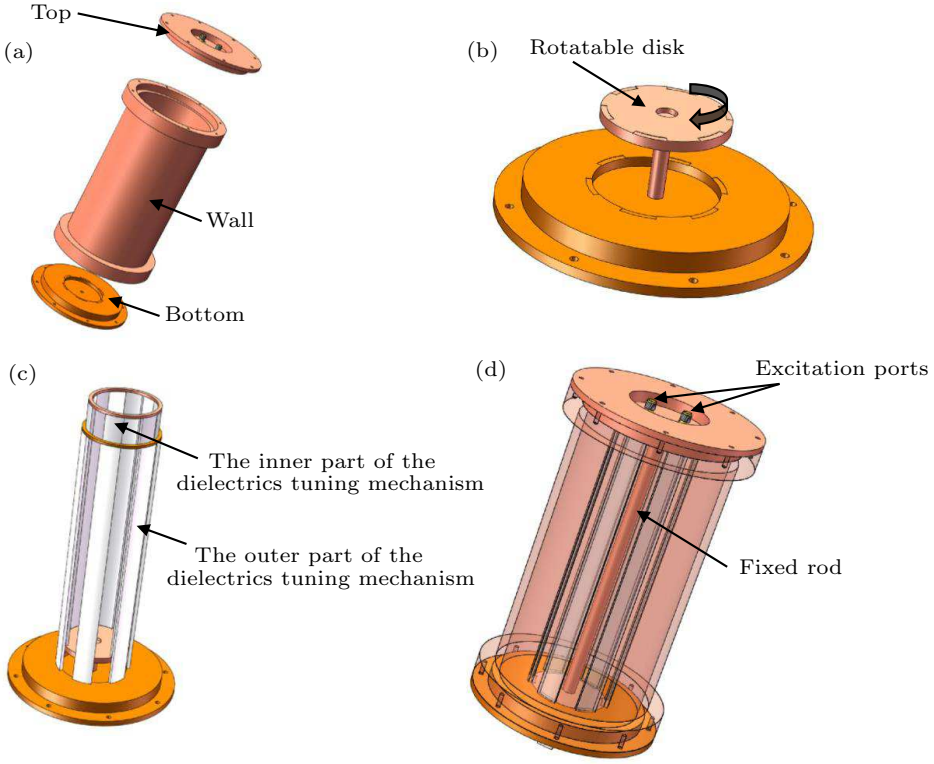


Fig. 9. Mechanical design model for the (a) metal enclosure, (b) rotatable disk embedded in the bottom endcap, (c) dielectric tuning mechanism, (d) central fixed rod and excitation ports of the microwave cavity.

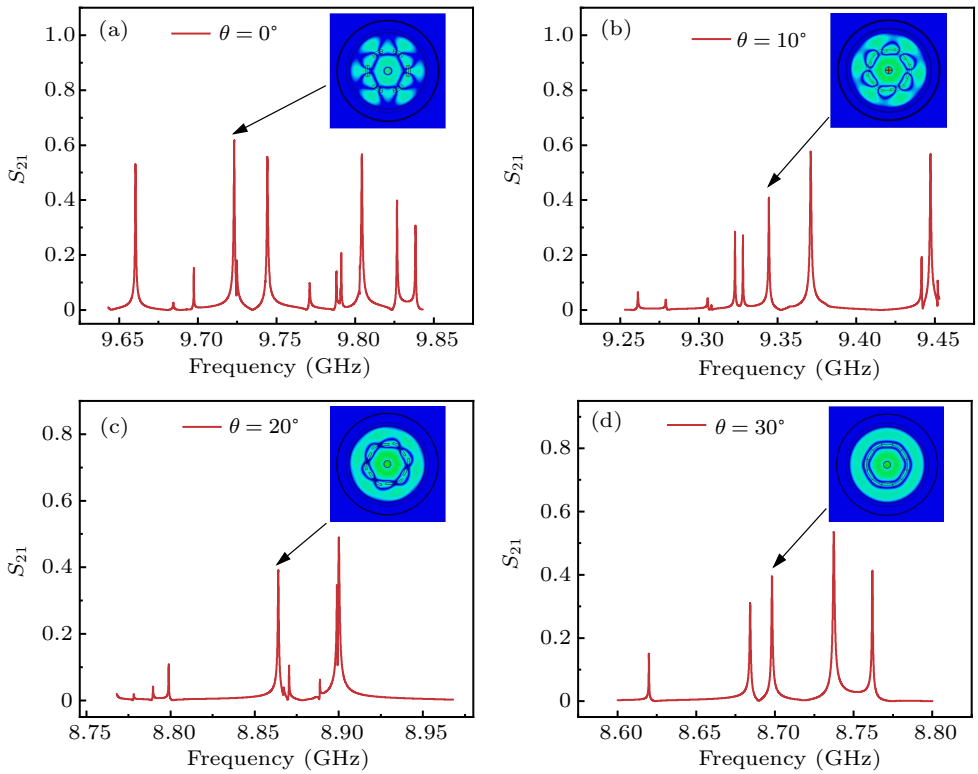


Fig. 10. Simulated transmission spectra of the mechanical design model of the microwave cavity corresponding to rotation angles of (a) 0°, (b) 10°, (c) 20°, and (d) 30° for inner dielectric pieces. The inset of each figure shows the electric field distribution of the microwave cavity corresponding to the TM_{030}-like mode resonance peaks.

Subsequently, the full-wave simulation was performed using the frequency domain solver of CST Studio Suite to predict the microwave response of the practical cavity. Figure 10 shows the transmission coefficient of the microwave cavity corresponding to different dielectric tuning mechanism rotation angles. The simulated results demonstrate that the resonant frequency of the novel design cavity operating in TM_{030}-like mode can be tuned from 9.726 GHz to 8.698 GHz by rotating the inner dielectrics from 0° to 30° relative to the outer part, thus verifying the feasibility of the scheme.

5. Conclusion

This paper proposed a novel design for the high-frequency microwave cavity in the haloscope. Benefitting from the rotatable dielectric pieces and the inserted metal rod in the center, the proposed design shows improvement in the effective volume of the high-order mode cavity. Besides, the tuning range of frequency can be significantly enlarged. The geometry parameters of the dielectric tuning mechanism were determined to maximize the FOMF through EM simulation. After completing the cavity design, a comparative investigation based on simulation was conducted to show the advantages of the novel design scheme over two previous schemes proposed in Refs. [11,15]. Remarkably, the FOMF can be elevated by more than three times, indicating that the haloscope with the cavity in novel design can efficiently scan a wider range of axion mass. Furthermore, the microwave response was evaluated by full-wave simulation of the mechanical design model. The evident variation of transmission spectra with rotation angles of dielectric pieces indicates the tunability of the cavity with the novel design, demonstrating the feasibility of the proposed design scheme. The novel design proposed in this paper paves the way for searching high-mass dark matter axion with high efficiency in the future.

Acknowledgements

Project supported in part by the Equipment Development Project for Scientific Research of the Chinese Academy of Sciences (Grant No. YJKYYQ20190049), the Innovation Program for Quantum Science and Technology (Grant No. 2021ZD0301800), and the National Key R&D Program of China (Grant No. 2022YFA1603904).

References

[1] Stecker F W and Shafi Q 1983 *Phys. Rev. Lett.* **50** 928
[2] Sikivie P 1983 *Phys. Rev. Lett.* **51** 1415
[3] Sikivie P 1985 *Phys. Rev. D* **32** 2988
[4] Hagmann C, Sikivie P, Sullivan N, Tanner D B and Cho S I 2015 *Rev. Sci. Instrum.* **61** 1076
[5] Asztalos S J, Carosi G, Hagmann C, Kinion D, Van Bibber K, Hotz M, Rosenberg L J, Rybka G, Hoskins J, Hwang J, Sikivie P, Tanner D B, Bradley R and Clarke J 2010 *Phys. Rev. Lett.* **104** 041301
[6] Braine T, Cervantes R, Crisosto N, Du N, Kimes S, Rosenberg L J, Rybka G, Yang J, Bowring D, Chou A S, Khatiwada R, Sonnenschein A, Wester W, Carosi G, Woollett N, Duffy L D, Bradley R, Boutan C, Jones M, LaRoque B H, Oblath N S, Taubman M S, Clarke J, Dove A, Eddins A, O'Kelley S R, Nawaz S, Siddiqi I, Stevenson N, Agrawal A, Dixit A V, Gleason J R, Jois S, Sikivie P, Solomon J A, Sullivan

N S, Tanner D B, Lentz E, Daw E J, Buckley J H, Harrington P M, Henriksen E A and Murch K W 2020 *Phys. Rev. Lett.* **124** 101303

[7] Hoskins J, Hwang J, Martin C, Sikivie P, Sullivan N S, Tanner D B, Hotz M, Rosenberg L J, Rybka G, Wagner A, Asztalos S J, Carosi G, Hagmann C, Kinion D, Van Bibber K, Bradley R and Clarke J 2011 *Phys. Rev. D* **84** 121302

[8] Khatiwada R, Bowring D, Chou A S, Sonnenschein A, Wester W, Mitchell D V, Braine T, Bartram C, Cervantes R, Crisosto N, Du N, Rosenberg L J, Rybka G, Yang J, Will D, Kimes S, Carosi G, Woollett N, Durham S, Duffy L D, Bradley R, Boutan C, Jones M, Laroque B H, Oblath N S, Taubman M S, Tedeschi J, Clarke J, Dove A, Hashim A, Siddiqi I, Stevenson N, Eddins A, O'Kelley S R, Nawaz S, Agrawal A, Dixit A V, Gleason J R, Jois S, Sikivie P, Sullivan N S, Tanner D B, Solomon J A, Lentz E, Daw E J, Perry M G, Buckley J H, Harrington P M, Henriksen E A, Murch K W and Hilton G C 2021 *Rev. Sci. Instrum.* **92** 124502

[9] Buschmann M, Foster J W and Safdi B R 2020 *Phys. Rev. Lett.* **124** 161103

[10] Klaer V B and Moore G D 2017 *J. Cosmol. Astropart. Phys.* **2017** 049

[11] Rapidis N M, Lewis S M and van Bibber K A 2019 *Rev. Sci. Instrum.* **90** 024706

[12] Kuo C L 2020 *J. Cosmol. Astropart. Phys.* **2020** 010

[13] Stern I, Chisholm A A, Hoskins J, Sikivie P, Sullivan N S, Tanner D B, Carosi G and van Bibber K 2015 *Rev. Sci. Instrum.* **86** 123305

[14] Jeong J, Youn S, Ahn S, Kim J E and Semertzidis Y K 2018 *Phys. Lett. B* **777** 412

[15] Kim J, Youn S, Jeong J, Chung W, Kwon O and Semertzidis Y K 2020 *J. Phys. G: Nucl. Part. Phys.* **47** 035203

[16] Read J I 2014 *J. Phys. G: Nucl. Part. Phys.* **41** 063101

[17] Alesini D, Braggio C, Carugno G, Crescini N, D'Agostino D, Di Gioacchino D, Di Vora R, Falferi P, Gambardella U, Gatti C, Iannone G, Ligi C, Lombardi A, Maccarrone G, Ortolan A, Pengo R, Pira C, Rettaroli A, Ruoso G, Taffarello L and Tocci S 2020 *Rev. Sci. Instrum.* **91** 094701

[18] CST Studio Suite 2021 December 2020 Dassault Systèmes Paris, France https://www.3ds.com/products/simulia/cst-studio-suite

[19] Youn S W 2017 *2nd Workshop on Microwave Cavities and Detectors for Axion Research*, January 10–13, 2017, California, USA